Improved Capacitor Using Amorphous RuO_2

David Evans
Evans Capacitor Company
72 Boyd Avenue
East Providence, RI 02914
401-434-5600

Dr. Jim Zheng
FAMU-FSU College of Engineering
2525 Pottsdamer St.
Tallahassee, FL 32310
850-487-6464

Dr. Scott Roberson
U.S. Air Force
Bldg. 432
306 W. Eglin Blvd.
Eglin AFB, FL 32542-6810
850-882-2006

Introduction

A balance exists between energy density and power capability for many systems that use and store energy. The energy density versus internal resistance relation is often times the key to developing a successful energy storage and delivery device for a particular application. Unfortunately, this relationship is often overlooked regarding electrochemical capacitor applications.

With energy storage materials, the ability to reduce the resistivity of the material while increasing the energy density can present a difficult problem. In most cases, raising a capacitor energy density reduces its power capability or vice versa, but rarely can both be optimized at once. For instance, many carbon-based double layer capacitor systems have high energy density, but they also posses a higher resistance than systems containing more electrically conductive materials.

To decrease the resistance, capacitors can be connected in parallel, but the resulting extra capacitance can be a detriment. In addition to the obvious effect of lower *useful* energy density, there are electrical performance penalties. Charging time is a function of total capacitance, for example, and extra capacitance means a longer charging time. For some capacitors to deliver the required pulse power, an oversized capacitor may be used to decrease internal resistance and hold the I R voltage drop within acceptable levels. In this case, a capacitor optimally fitted to the

Presented to the 9th International Seminar on Double Layer Capacitors and Similar Energy Storage Devices, December 6-8, Deerfield Beach, Florida.

application in terms of capacitance, although lower in energy density, can still be the best choice. Less capacitance also generally has the added benefits of lower leakage current and lower cost.

As has been demonstrated with many carbon systems, the ability to produce higher surface areas and hence a higher double layer capacitance is continually increasing. As mentioned above, high energy density alone cannot satisfy all the requirements for a list of capacitor applications. It is possible to lower the resistance for a given capacitance by decreasing the electrode thickness in electrochemical capacitors, but this scheme inevitably reduces the ratio of active/total mass and causes a lowering of the energy density. Another approach is to use a more conductive electrode material. The transition metal oxides and nitrides are promising as low resistance electrode materials more suitable for pulse power applications. They can simultaneously offer higher energy density and reduced resistance compared to carbon.

In this effort, the fabrication of low resistance, high energy density devices is being investigated. The devices being developed in this effort are designed for pulse power and short duration, high output situations. In addition, these devices will be investigated under shock loads to 10,000 g's to determine their performance.

Three different high performance capacitor technologies using state-of-the-art electrode material based on amorphous $RuO_2.xH_2O$ were investigated. Each of the three capacitor types has certain advantages which tend to suit different applications. For example, the particulate amorphous 10V $RuO_2.xH_2O$ symmetric shock-hardened capacitor prototype has almost three times the energy density , and 1/3 the time constant of the Capattery® carbon symmetric shock-hardened capacitor. The shock-hardened tantalum Hybrid® capacitor prototypes are single cell 25 and 7.5V units. The cathode used is an amorphous $RuO_2.xH_2O$ film on tantalum foil. While the energy density of these units are < 10% that of the symmetric amorphous $RuO_2.xH_2O$ prototype, the frequency response is 100 times higher. While the low specific gravity of aluminum suits it for shock -hardened capacitor applications, the main attractions are its low cost compared to tantalum and the near-term potential for high cell voltages.

Experimental

Particulate Amorphous RuO_2 Electrode Material Preparation

A batch of amorphous ruthenium dioxide powder material was prepared by annealing commercially available hydrous ruthenium dioxide powders at the optimal temperature. At the optimal temperature, the maximum value of specific capacitance was obtained. It was found that the optimal temperature was just below the temperature at which the crystalline phase started to be formed.

A batch of composite electrode material, which comprised 80 wt.% amorphous ruthenium oxide powder and 20 wt.% activated carbon black, was prepared and delivered to Evans. The activated carbon black used in this composite electrode material was Black Pearls-2000 from Cabot.

Several trials were made to determine the best electrode material / electrolyte ratio. In each trial, approximately 5g of the composite electrode material, powder was placed in a ~100 cc screw-top polypropylene cup. Electrolyte (38wt% H_2SO_4) was added until a paste was formed. The electrode mixture with the best mechanical properties for electrode fabrication had a weight composition of 1 part powder : 1.5 parts electrolyte. The materials were mixed by hand using a Teflon coated spatula.

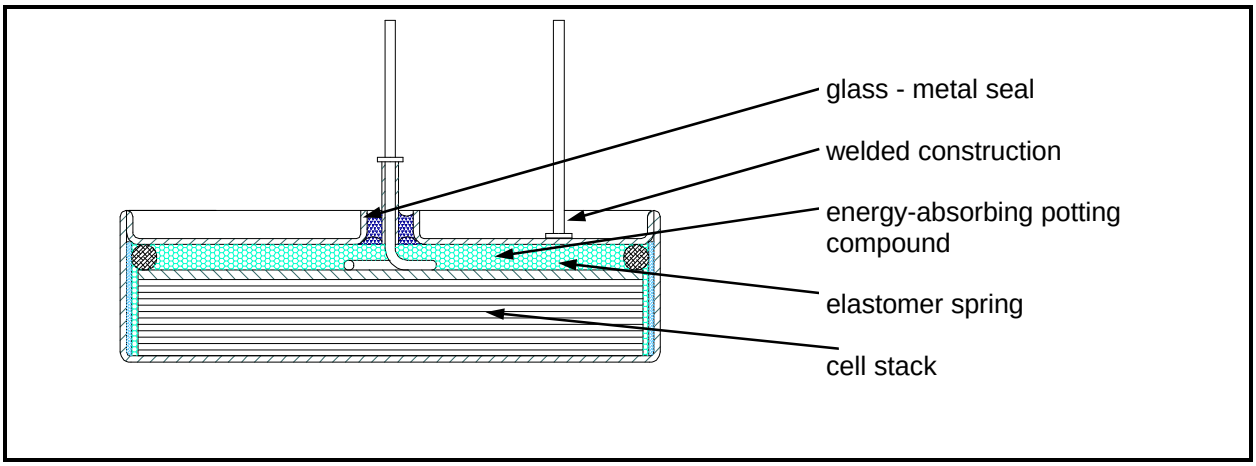

Figure 1. Drawing of the 12-cell shock-hardened symmetric amorphous RuO2.xH2O prototype capacitor showing details of the internal construction. Upon acceleration, small motion of the cell stack relative to the case causes the potting compound to flow. This, in turn, absorbs energy, cushioning the shock. The unit is designed to allow the motion under the influence of the elastomer spring without effecting electrical performance.

Preparation of Ruthenium Oxide Film Electrode

The precursor for growth of amorphous ruthenium oxide film was made as follows:

$$RuCl_3 + 3Na(OC_2H_5) \rightarrow Ru(OC_2H_5)_3 + 3NaCl$$

This reaction occurred in the ethanol solvent at the temperature of 78 °C, which is the boiling temperature of ethanol. When the reaction was completed, the ruthenium ethoxide ($Ru(OC_2H_5)_3$) dissolved, and NaCl precipitated in the ethanol solvent.

One surface of the as received tantalum foil (0.05mm, Cabot) was abraded with a brush made of palladium wire. This was followed by vacuum heat treatment at 900°C for ½ hour. This procedure improves adhesion and greatly diminishes the contact resistance of the tantalum foil surface. This treated tantalum foil was used as the substrate, which was heated to a desired temperature. Next, the ruthenium ethoxide solution was applied to the substrate surface using an

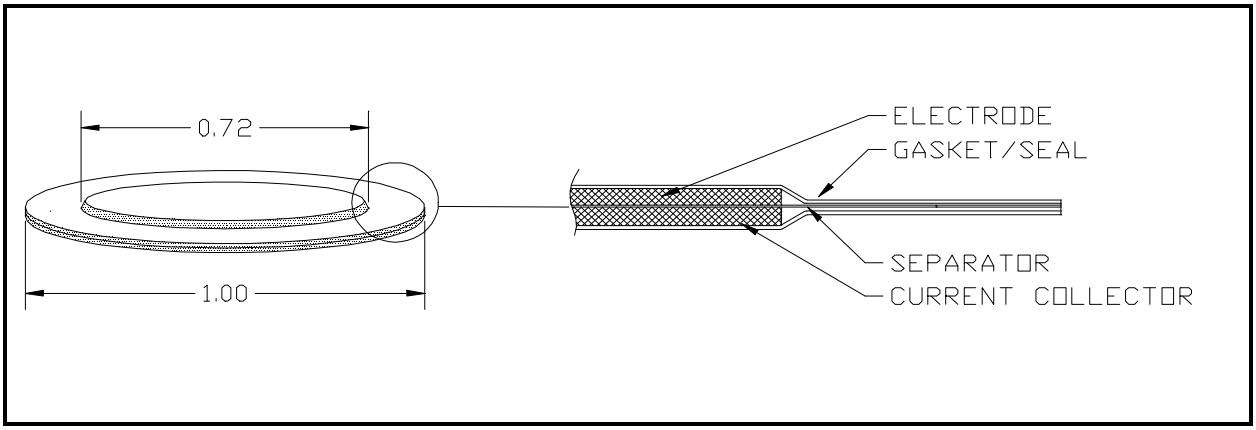

Figure 2. Cell cross-section view

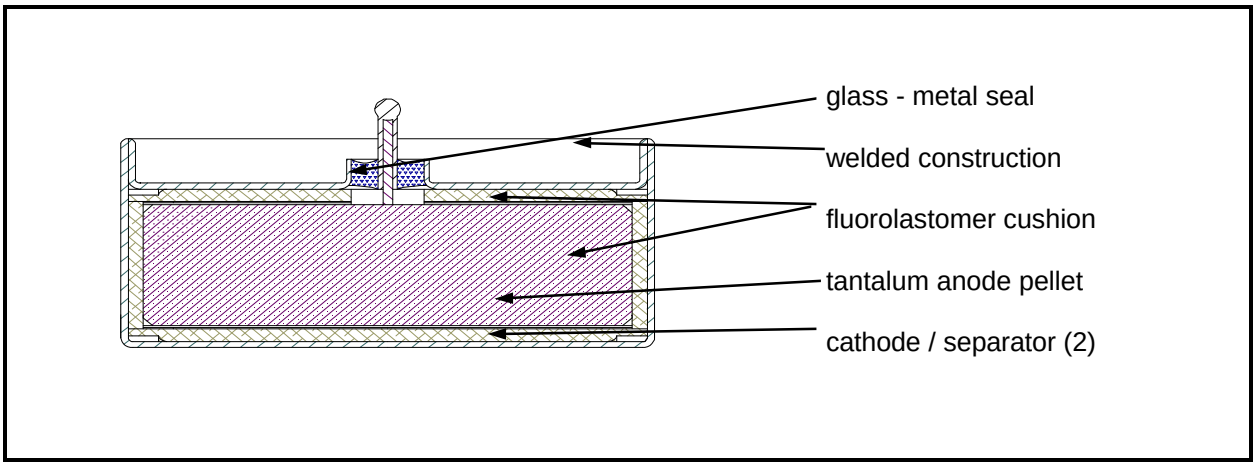

Figure 3. Drawing of the 25 V shock-hardened hermetic tantalum prototype capacitor showing details of internal construction. Upon acceleration , this unit absorbs mechanical energy due to the motion of the anode relative to the case. This motion, governed by the elastomer cushion, forces internal electrolyte flow, dissipating energy and reducing the peak load.

airbrush. After each coating, the film electrode was dipped into boiling water in order to remove any material that was incompletely oxidized and any residual NaCl.

Symmetric RuO_2 Electrochemical Capacitor

A twelve-cell shock-hardened, symmetric particulate RuO_2 electrochemical capacitor was constructed. Figure 1 shows a cross-section view and important features of the unit. A drawing of the cell is shown in Figure 2. Cell symmetry is important to electrical performance, and the amount of electrode material used was controlled by volume. The volume was 0.034 cm^3/ electrode. The electrode paste was applied to the current collector. This formed a smooth, flat electrode 0.004 to 0.005 inches thick. Gasket – Current Collector assemblies were pre-made in a punch-and-die operation. Two electrode – gasket – collector assemblies (half-cells) were made for each cell. A single pre-punched separator was adhered to the exposed gasket surface of one half-cell. Finally, the two half-cells were mated.

The current collector used in this work was 0.002" high-carbon conductive film manufactured by Rexam Graphics of S. Hadley, MA. The separator used in this work was 0.001" Celgard microporous polypropylene/polyethylene separator manufactured by Hoecst Celanese. The gasket/seal used was a 0.0005" thick pressure sensitive acrylic/polyester adhesive film.

Shock-Hardened Tantalum Hybrid® Capacitor

A 25 V and a 7.5 V shock-hardened hermetic tantalum Hybrid® electrochemical-electrolytic capacitor was constructed. Both units had a capacitance of 0.034 F at 120 Hz. Figure 3 shows a cross-section view and important features of these units. Capacitor grade tantalum powder was pressed in existing tooling to form a green compact 0.960 inches in diameter. The 25 V capacitor anode was 0.281 inches thick and weighed 18g. The 7.5 V capacitor anode was 0.090 inches thick.and weighed 5.5g. Next, the compacts were sintered in vacuum at about 1325°C for 1/2 hour. After cooling, the sintered pellets were immersed in an electrolyte solution containing 0.1% H_3PO_4, maintained at 85°C. The tantalum pellets were connected to the positive

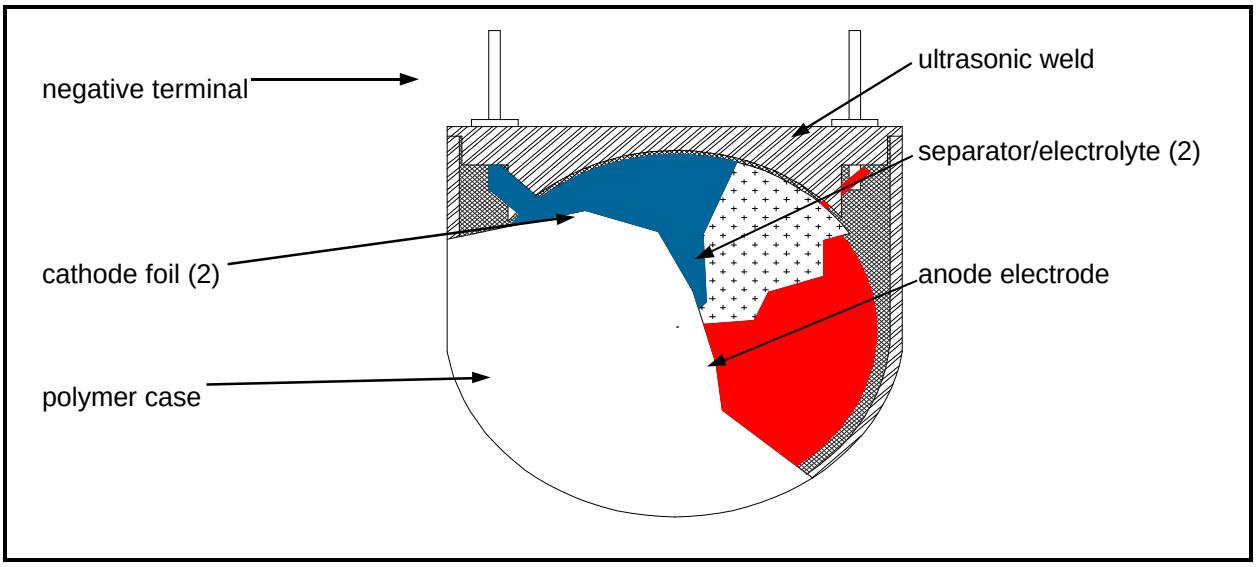

Figure 4. Cut-away view of aluminum hybrid electrochemical-electrolytic capacitor in polymer case. The packaging used is an adaptation of tantalum Hybrid® capacitor case components.

terminal of a power supply. The negative terminal was connected to a strip of stainless steel immersed in the electrolyte close to the pellets. Ta_2O_5, formed electrochemically on the surface of the tantalum pellets by this process serves as the capacitor dielectric. Current, limited to 50 mA/g was supplied until 1.25 times the intended working cell voltage was reached at a current < 10 mA. The pellets were then cleaned in boiling DI water, and the process repeated in a 38% H_2SO_4 solution at 85°C. Instead of stainless steel, a tantalum cathode was used. Again, the voltage was applied, and the current finally fell to the < 100 **m**A range.

Each of the components was assembled according to the drawing in Figure 3. Tabs cut in the cathode foils extended to the case rim. A double thickness of glass-polypropylene separator (Hollingsworth and Vose) was inserted between the anode and each cathode foil. The rim of the case was welded using existing tooling and procedures. 38% H_2SO_4 electrolyte solution was added by vacuum fill through the feed through tube, which was subsequently welded shut. Leads were attached to the case and feed through by resistance welding.

Aluminum Hybrid® Capacitor

A 28 V aluminum Hybrid® electrochemical-electrolytic capacitor was constructed. Figure 4 is a drawing of this unit. Etched pure aluminum, electrochemically oxidized at 35 volts was used as the anode electrode. The dimensions of the anode were 1.30 inches diameter and 0.29 inch tall. The total anode weight was 8.0 g.

The electrolyte used for this capacitor was a pre-formulated commercially available ethylene glycol-based material. This electrolyte was designed for use in aluminum electrolytic capacitors. As reported by the manufacturer, it had a conductivity of 12mS/cm, and a pH of 7.5 at 30°C.

The anode was dipped in electrolyte. The components were assembled according to the drawing in Figure 4. The aluminum anode was connected to the positive terminal of the capacitor by resistance welding its contact wire to the terminal feedthrough. Cathode foils were also attached by welding. Additional electrolyte was added to the package prior its final closure by

ultrasonic welding.

Shock Testing the Capacitors

The 7.5 V, 34 mF, 50 mohm Evans Hybrid® Capacitor was connected to an IES Model 54 4 channel data recorder and loaded into a stainless steel canister in glass beads and preloaded to 5,000 psi. The capacitor was monitored using two channels: (1) monitoring the voltage output on the capacitor and (2) the output of the capacitor through a 5V 60 mA voltage regulator. Theses two outputs were chosen to evaluate both the shock survivability and the performance during shock of the device. The canister was then sealed and loaded into a ballistic and launched at high velocity out of a howitzer gun where it impacted a concrete target. The ballistic was recovered and the data was downloaded at a later time. The shock spectrum was monitored using an Endevco 7270 – 60Kg accelerometer which was also connected to the Model 54 IES recorder.

Results and Discussion

Ruthenium Oxide Powder and Composite Materials

Figure 5 shows a cyclic voltammagram measured from an electrode made with amorphous ruthenium dioxide powder at a voltage scan rate of 2 mV/sec. The specific capacitance was about 660 F/g that was about 92% of that measured from previous electrode materials prepared by the sol-gel method. However, the new method is simplifies procedures for making electrode materials and is suitable for mass production.

The most significant advantage of amorphous ruthenium oxide electrode is the high specific capacitance due to the proton intercalation process. However, it was found that the maximum power density of the electrochemical capacitors made with amorphous ruthenium oxide

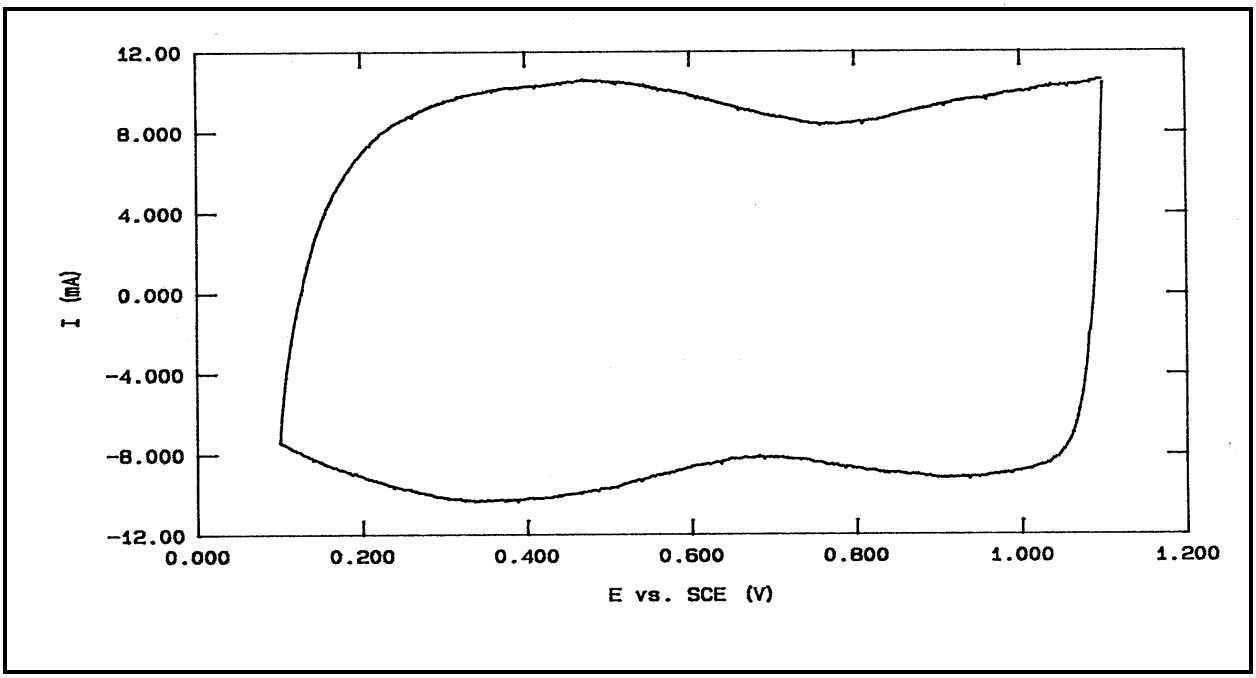

Figure 5. Cyclic voltammgram of amorphous ruthenium oxide electrode in 38 wt.% H_2SO_4 electrolyte at a voltage scan rate of 2 mV/sec. The electrode was made with 6.86 mg of ruthenium dioxide powder and 0.34 mg of Teflon as binder.

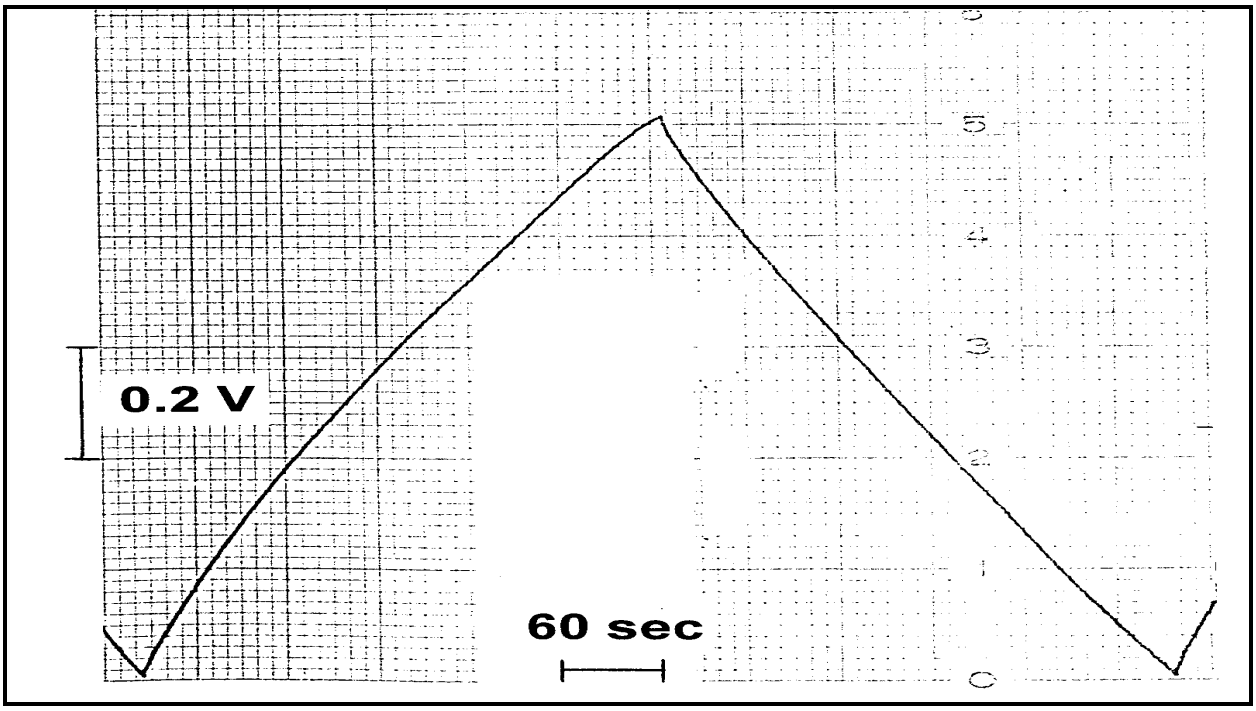

Figure 6. DC charge and discharge curve of a symmetrical capacitor with two film electrodes in H_2SO_4 electrolyte. The current was 2 mA. The voltage was 0-1 V.

is low due to the ion depletion in the electrolyte. When highly porous activated carbon black was mixed with amorphous ruthenium oxide powder to form composite material, the electrolyte absorbed inside electrode increased; therefore, the maximum power density of the electrochemical capacitor was improved significantly. The specific capacitance of the composite electrode material was about 570 F/g.

Symmetric RuO_2 Electrochemical Capacitor

The twelve cells used in the symmetric RuO_2 electrochemical capacitor were selected from a larger group in order to reduce cell to cell variation. Electrical Impedance Spectroscopy (EIS) measurements were made on each cell in the larger group. These measurements were made with a Gamry Instruments CMS-100 system. All data were taken at 0V and room temperature. The measurement signal was 1mV, ac. Data from these measurements are presented in Figures 10 and 11. The same data for the twelve cells selected are presented in Figures 12 and 13. From this data on individual cells, the performance of a 12-cell series stack could be predicted. Predicted Bode capacitance and resistance are shown in Figures 14 and 15. EIS was used to evaluate the 12-cell capacitor. Figures 14 - 16 show Bode capacitance, resistance, and phase angle. Figure 17 is a Nyquist plot showing typical impedance behavior of an electrochemical capacitor with thin porous electrodes. The "dc" capacitance was about 0.37 F and the ESR at 1kHz was 0.43 ohms. The RC time constant is therefore 0.160 s, which is quite low for symmetric capacitors with electrodes made from particulate material.

Ruthenium Oxide Film Electrode

The traditional method of making ruthenium oxide film starts with $RuCl_3$ precursor. Because the chloride precursor can be thermally decomposed at temperatures above 300°C, The

Figure 7. Electrical impedance behavior of a typical symmetric test cell using improved RuO_2 film on pre-treated tantalum foil. Note that this gives the performance of two electrodes in series. In the intended application in a hybrid capacitor where only a single electrode is needed,the impedance (z' and z") would be 1/2 the value shown.

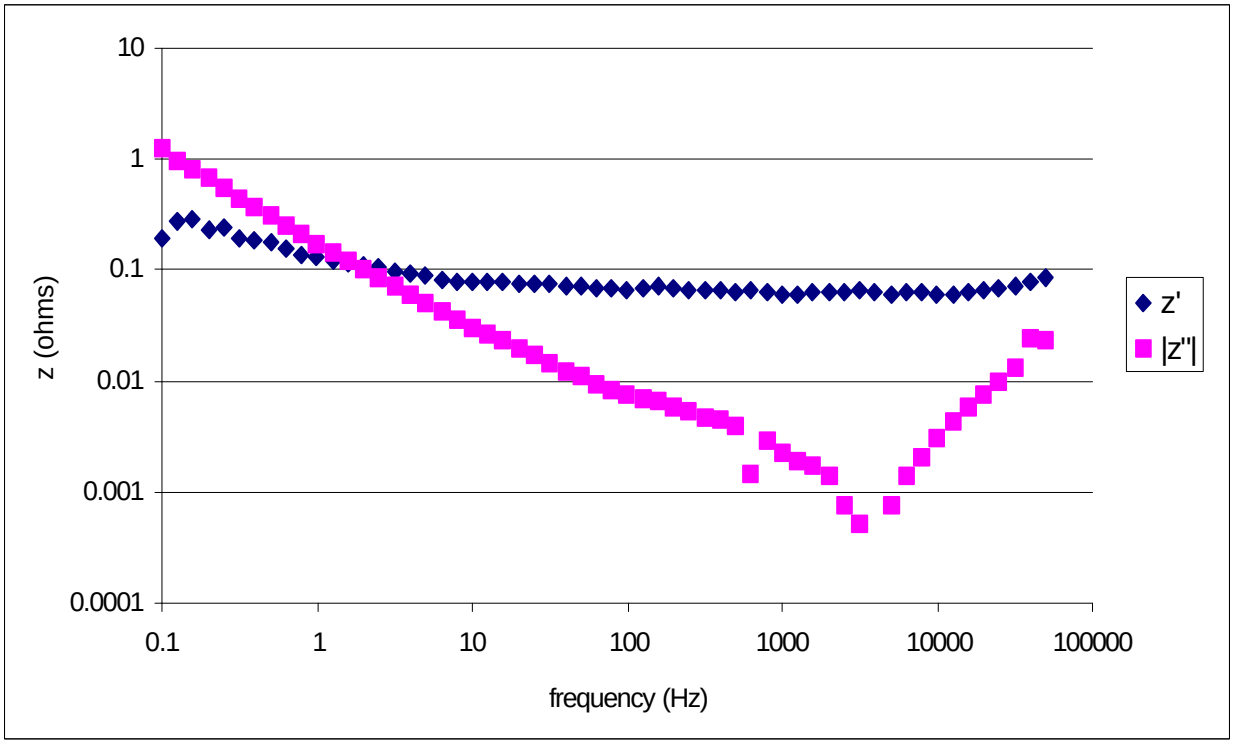

ruthenium oxide film is usually grown at high temperatures (300-500°C). At such high temperature, crystalline ruthenium oxide film is formed. However, in this project, we used new precursor of $Ru(OC_2H_5)_3$, which could be thermal decomposed at the temperature as low as 100°C. At such low temperature, amorphous ruthenium oxide was able to form. The major advantage of amorphous ruthenium oxide is that the specific capacitance is much higher than that from crystalline ruthenium oxide.

Figure 6 shows a dc charge/discharge curve under a constant current of 2 mA. During tests, a symmetrical capacitor was made with two film electrodes in 0.5 mol H_2SO_4 solution as the electrolyte. The size of each film electrode was 1.56 cm^2. The capacitor was charged and discharged in the voltage range from 0 to 1 V. From Figure 8, the total capacitance was calculated to be about 0.66 F, which was corresponding to an interfacial capacitance of 0.85 F/cm^2 or 5.5 F/in^2 for single electrode. This value was over 20 times higher than that proposed in the phase I proposal.

Figure 7 shows typical electrical impedance measurements for a symmetric cell made from the RuO_2 film material. The area of each electrode was 5 cm^2. The point where z' intersects z" is the frequency where the phase angle is -45°, and this occurs at 1.6 Hz. The frequency of self resonance, where z" = 0 is at about 3500 Hz.

Shock-Hardened Tantalum Hybrid® Capacitor

Electrical Impedance Spectroscopy (EIS) measurements were made on the 25 V shock-hardened tantalum Hybrid® capacitor. These measurements were made with a Gamry

Table 1. Comparative results are summarized below.

Description	Voltage	Capacitance (farads)	ESR (ohms) @1kHz	J/g	J/cm3	RC (ms)
RuO_2 Symmetric	10	0.37 (dc)	0.43	0.56	2.38	150
Tantalum Hybrid 1	25	0.034 (120Hz)	0.049	0.45	1.36	1.7
Tantalum Hybrid 2	7.5	0.034 (120Hz)	0.050	0.042	0.19	1.7
Aluminum Hybrid	28	0.023 (dc)	0.99	0.35	0.59	23

Instruments CMS-100 system. All data were taken at 0V and room temperature. The measurement signal was 1mV, ac. Data from these measurements are presented in Figures 18-21. The capacitance of this device is 0.034 F @ 120 Hz, and 0.070 F at 1 Hz. The capacitor weighs 40 .8 g. Its dimensions are 0.52 inch high x 1.1 inch diameter.

Aluminum Hybrid® Capacitor

EIS measurements were made on the 28 V shock-hardened aluminum Hybrid® capacitor. All data were taken at 0V and room temperature. The measurement signal was 1mV, ac. Data from these measurements are presented in Figures 22-24. The ac impedance behavior of this capacitor is highly non-ideal with respect to similar measurements made on tantalum capacitors with pellet anode structures. Anode geometry and electrolyte resistivity are undoubtedly playing a major role.

The device capacitance (0.023 F) is higher than the expected anode capacitance (0.018 F) using numbers from the manufacturer, possibly because the anode material capacitance measurement method and cell used by the manufacturer differs significantly from the cell built and measured in this work. The ESR was 0.99 ohms. The RC time constant is therefore 23 ms. The capacitor weighs 25.1 g. Its dimensions are 0.38 inch high x 1.6 inch diameter.

Figure 25 shows voltage and current vs. time for charge-discharge cycling at 300 mA. The capacitance can be calculated as 0.024 F, which is in close agreement with the value of 0.023 F determined by EIS.

Shock Test Results

In addition to electrical evaluations performed at Evans Capacitor, the 7.5 V, 34 mF, 50 mohm capacitor was also evaluated for performance in high shock applications, such as concrete penetration tests mentioned previously. The results of one of these tests are shown in Figure 8. The bottom graph is a plot of the g loading (deceleration) versus time. The lighter colored trace is the raw, unfiltered data where as the darker line is the data filtered at 2 kHz. As can be seen from the bottom graph, the capacitor experienced g loads up to 27 kg (2 KHz). The negative deceleration (acceleration) part of the trace to 30 msec is the gun acceleration. This is followed by mechanical ringing due to the exit of the ballistic from the gun barrel, concrete target impact at 38 msec and then another impact on an unknown object at 55 msec. The corresponding capacitor

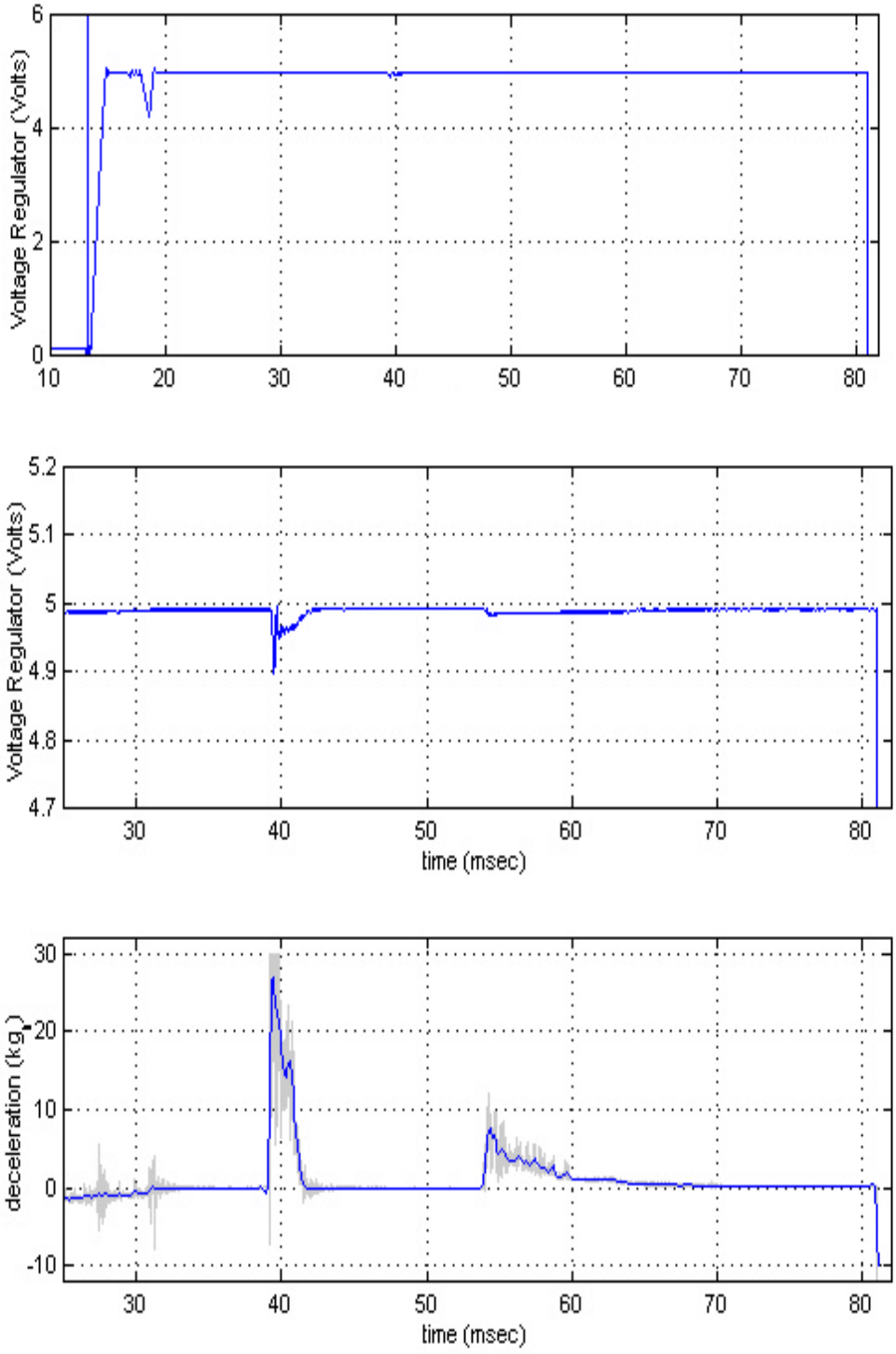

Figure 8. The output of the 7.5 V, 34 mF, 50 mohm Evans tantalum Hybrid® Capacitor. The bottom figure is the deceleration profile of the test , while the top two figures are output of the capacitor through a 5V , 60 mA regulated circuit. These figures indicate that there is very little voltage fluctuation on the circuit during testing under extreme shock loading.

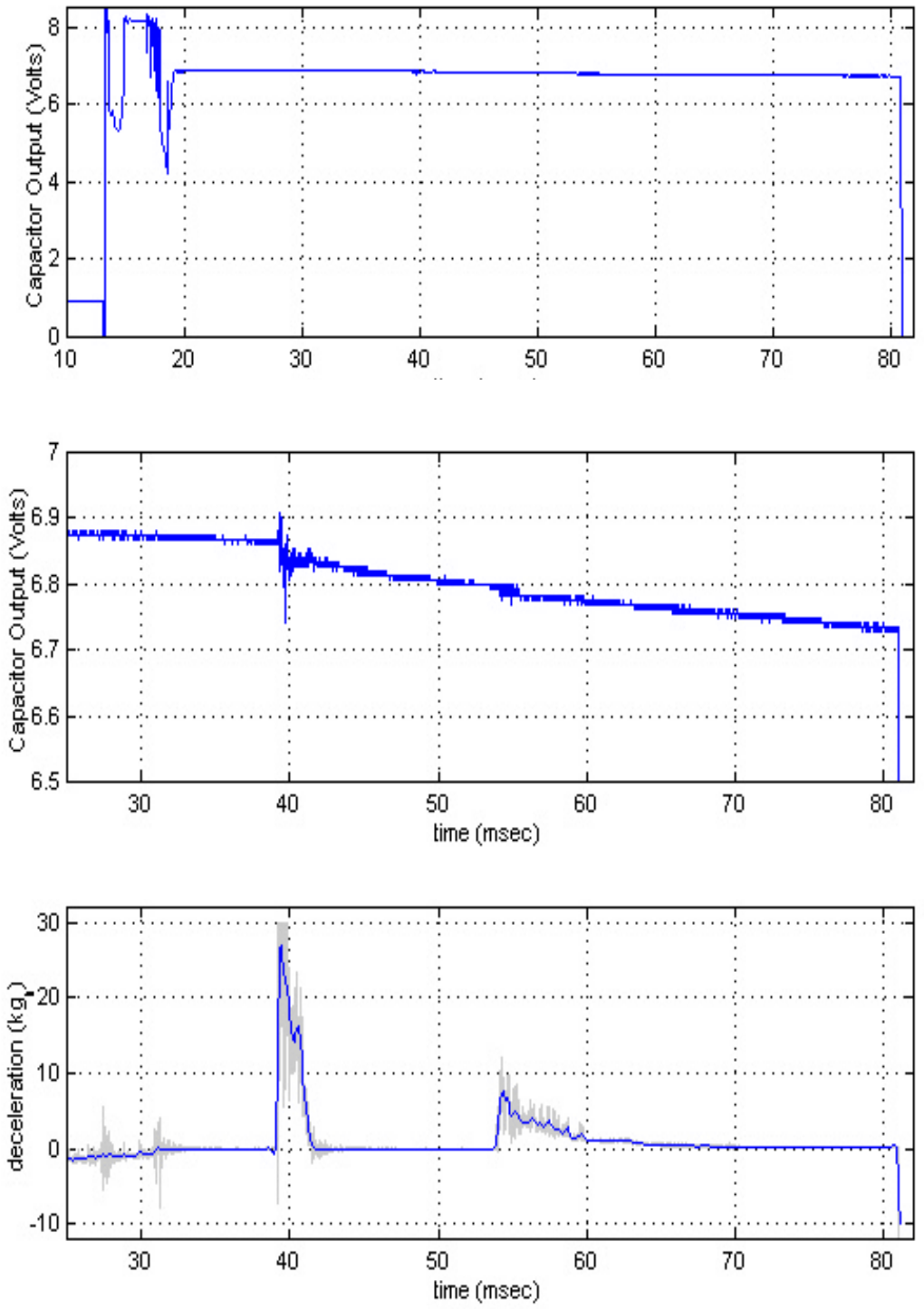

Figure 9. The output of the 7.5 V, 34 mF, 50 mohm Evans tantalum Hybrid® Capacitor. The bottom figure is the deceleration profile of the test , while the top two figures are the voltage on the capacitor during the test These figures indicate that there is only a small voltage drop on the capacitor during the extreme shock loading.

output from the 5V, voltage regulator is shown in the two figures above. The top figure indicates that the output of the capacitor through the 5 V regulator is constant during the test, which indicates that there was no damage to the capacitor or voltage dropout due to the shock level. The variations in voltage up to 20 msec are most likely due to the regulator warm up and turn on as the voltage recovers to 5 V. The middle figure is a more detailed view of the voltage regulator output indicating that at 40 msec there was a slight drop of 0.1 V on the regulator output. However, this is most likely due to the voltage regulator. This can be demonstrated by looking at Figure 9 where the actual voltage of the capacitor is plotted against time for the same shock spectrum. The bottom figure is the same as described above and the top figure is a plot of the voltage on the capacitor during the shock event. As can be seen the voltage on the capacitor at 40 msec only drops 0.2 V (max) and this voltage is still above the minimum required to operate the voltage regulator and is quite low for a shock test of this nature. Thus, it is most likely that the voltage fluctuation in Figure 8 is due to the voltage regulator itself and not the capacitor. As can also be seen from Figure 9, the voltage on the capacitor only drops 0.2 V during the entire test. This 0.2-Volt drop occurred while operating the 60 mA, 5V regulator circuit, thus there is very little voltage drop due to the shock load on the capacitor.

Conclusion

The three capacitors built under this project and delivered to the Air Force incorporate the benefits of amorphous RuO2 in the forms of particulate and film bound on tantalum foil. Both capacitor types, the symmetric and the hybrid are of great commercial interest with respect to both the military and private sector. In combination, they cover a broad spectrum, from dc to high-frequency (1 kHz) applications.

The properties of the aluminum capacitor would be improved by development of a lower resistivity electrolyte and inexpensive cathode plates with enhanced contact to the cathode material. Already, the energy density of the aluminum hybrid prototypes at least a factor of five better than aluminum electrolytic capacitors. Considerable potential now exists for applications of large numbers of these units if improvements are incorporated.

The tantalum symmetric and tantalum hybrid capacitors are technologically ready to market for military applications, and at this time have been successfully tested by the Air Force in a high-shock environment. Further effort is needed in characterizing performance and life testing these capacitors.

Acknowlegement

This work was partially supported by a grant from the:

Small Business Technology Transfer Program (DoD)
Air Force Research Laboratory
Bldg. 13, 101 West Eglin Blvd.
Eglin AFB, FL 32542-6810

Issued by AFRL/MNK under
contract number: F08630-98-C-0074

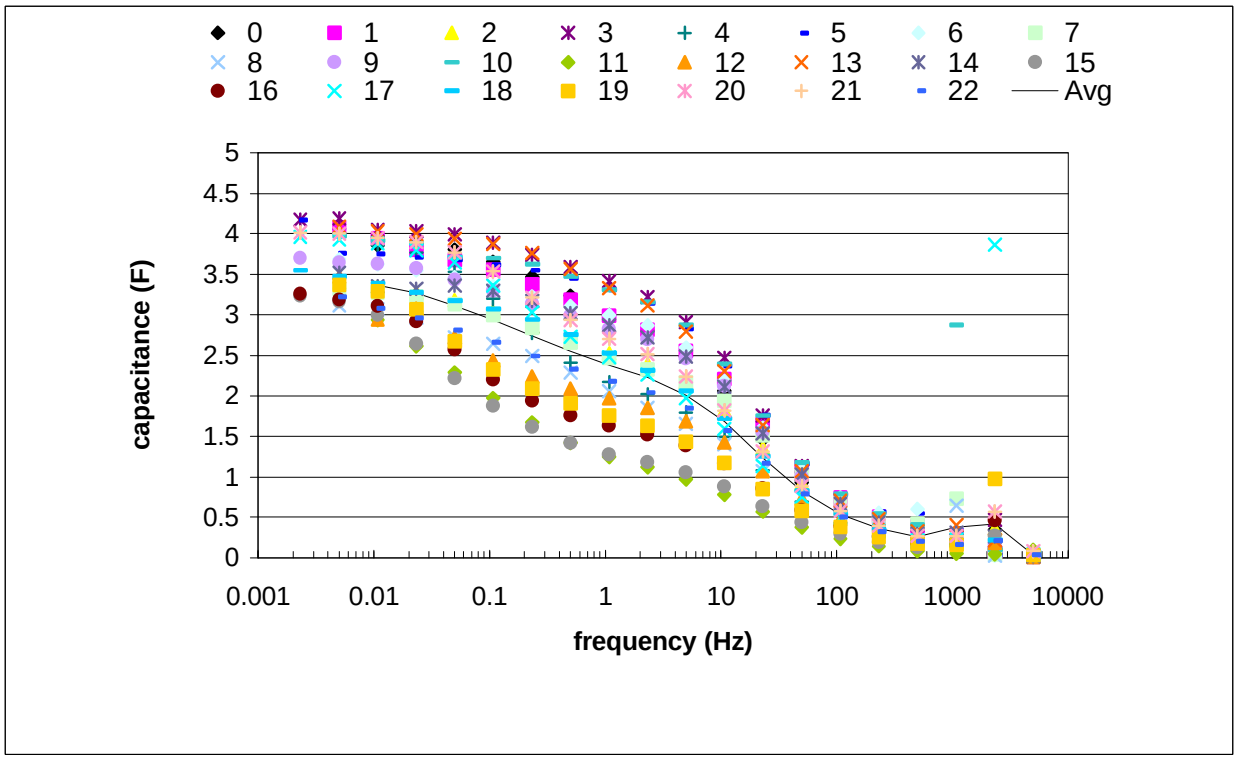

Figure 10. Capacitance vs. frequency for symmetric particulate amorphous RuO_2 cells.

Figure 11.Resistance vs. frequency for symmetric particulate amorphous RuO_2 cells.

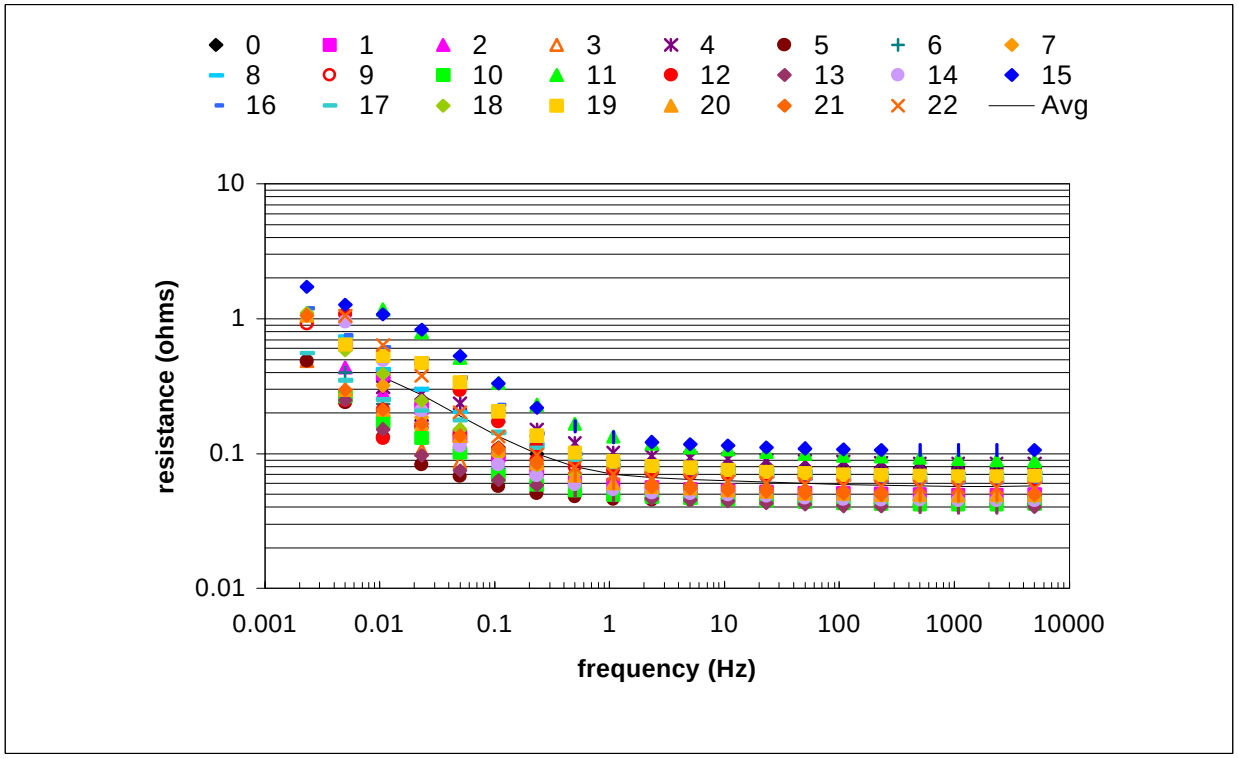

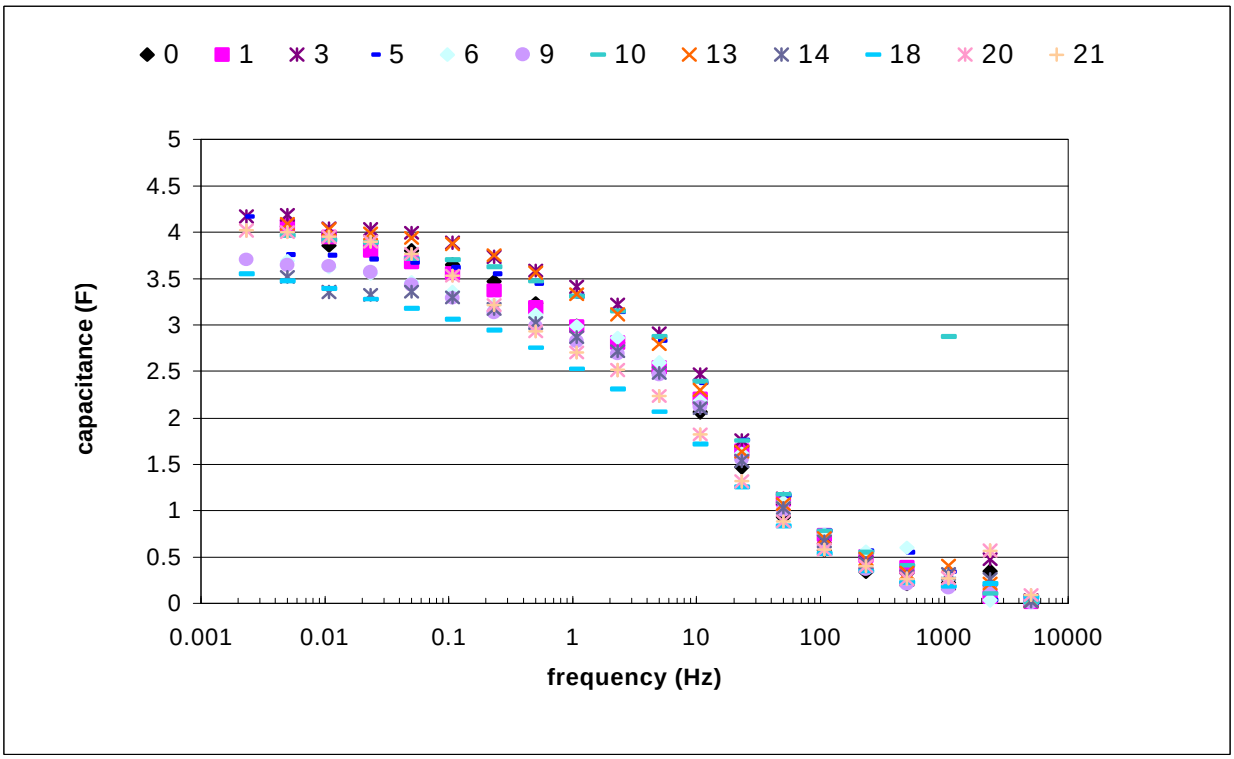

Figure 12. Capacitance vs. frequency for the twelve symmetric particulate amorphous RuO_2 cells used in the shock-hardened capacitor prototype.

Figure 13. Resistance vs. frequency for the twelve symmetric particulate amorphous RuO_2 cells used in the shock-hardened capacitor prototype.

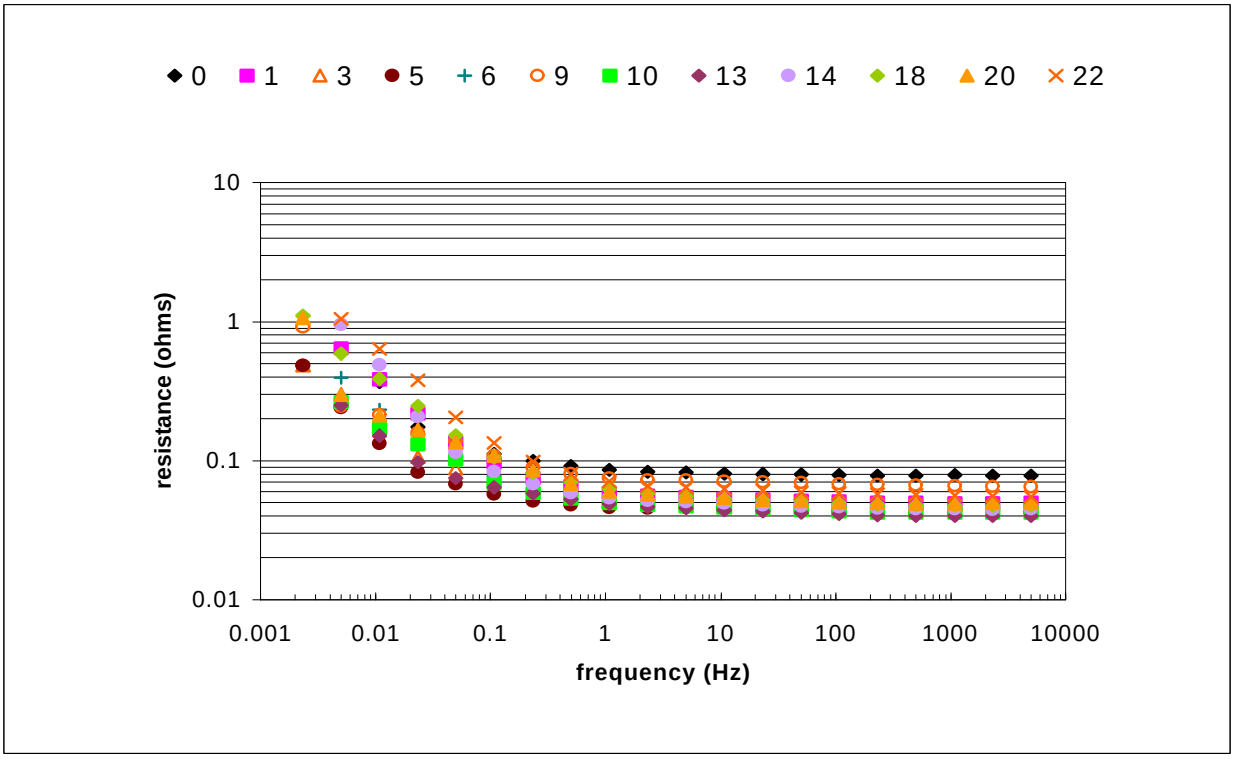

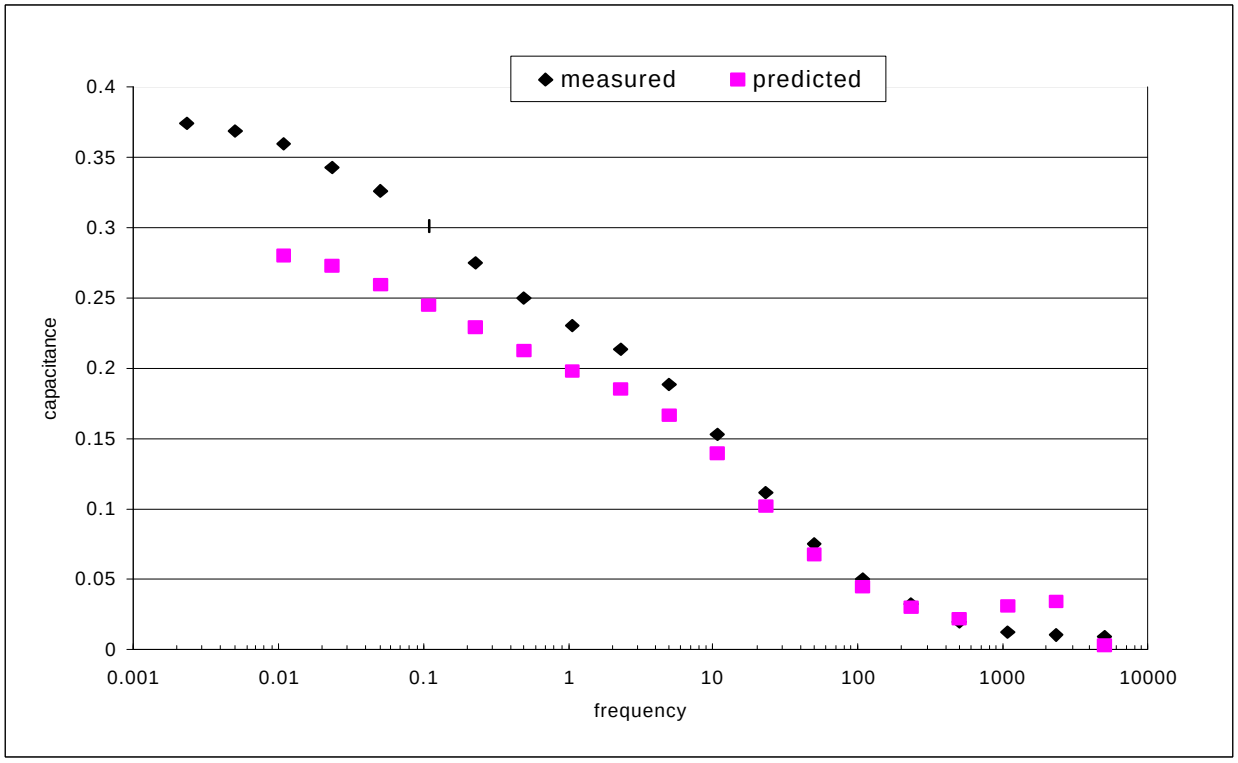

Figure 14 (above) and Figure 15 (below) show the capacitance and resistance vs. frequency for the twelve-cell symmetric particulate amorphous RuO_2 shock-hardened capacitor prototype. Predicted results are based on the average results of individual cells in a theoretical capacitor according to Ohm's Law. That the prototype capacitor performed better than predicted may be attributed to more axial compression of the cell and lower contact resistance than in the cell measurement fixture.

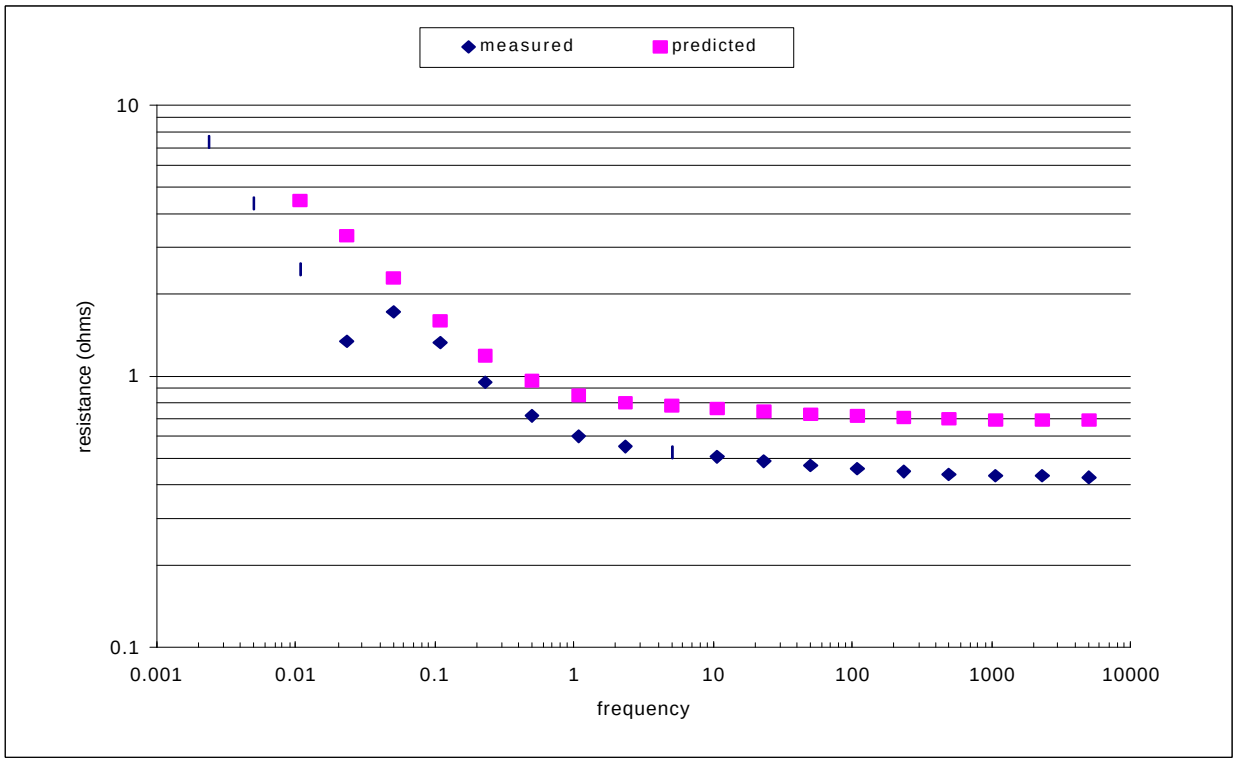

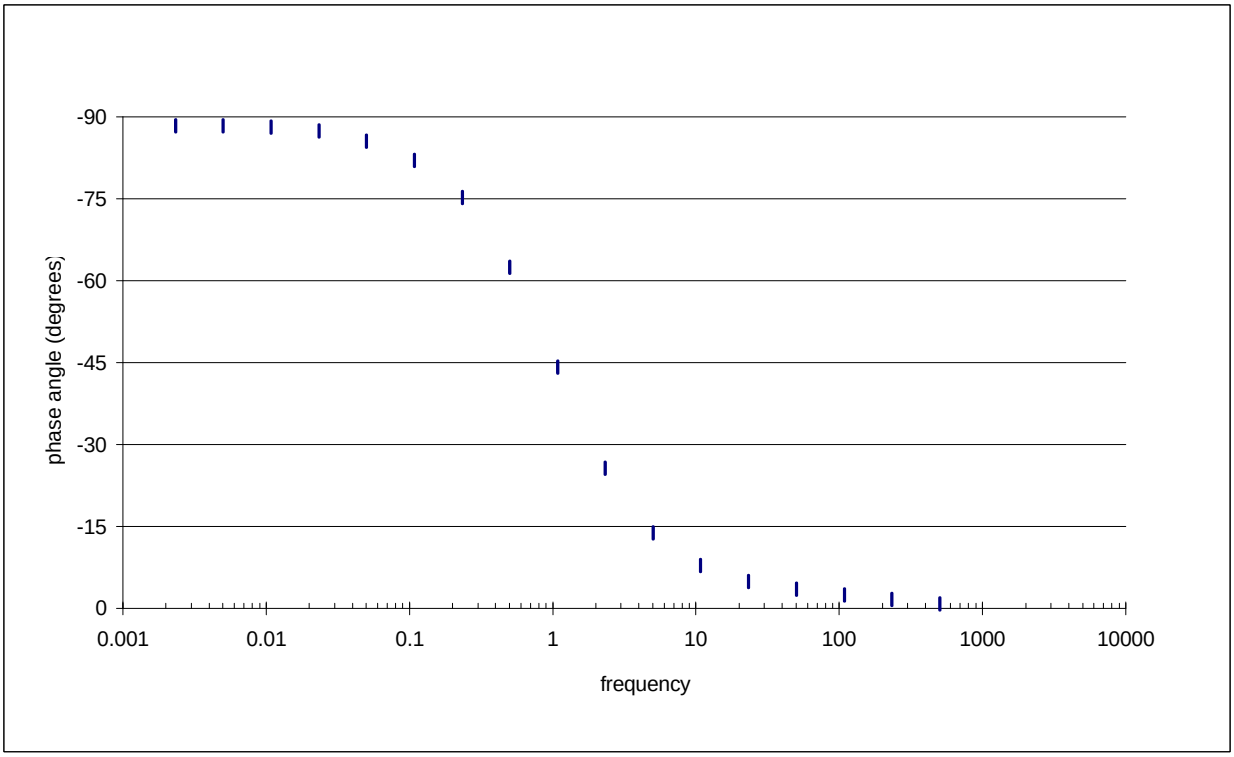

Figure 16. Phase angle vs. frequency for the twelve-cell symmetric particulate amorphous RuO_2 shock-hardened capacitor prototype.

Figure 17. Nyquist plot of the impedance data for the twelve-cell symmetric particulate amorphous RuO_2 shock-hardened capacitor prototype.

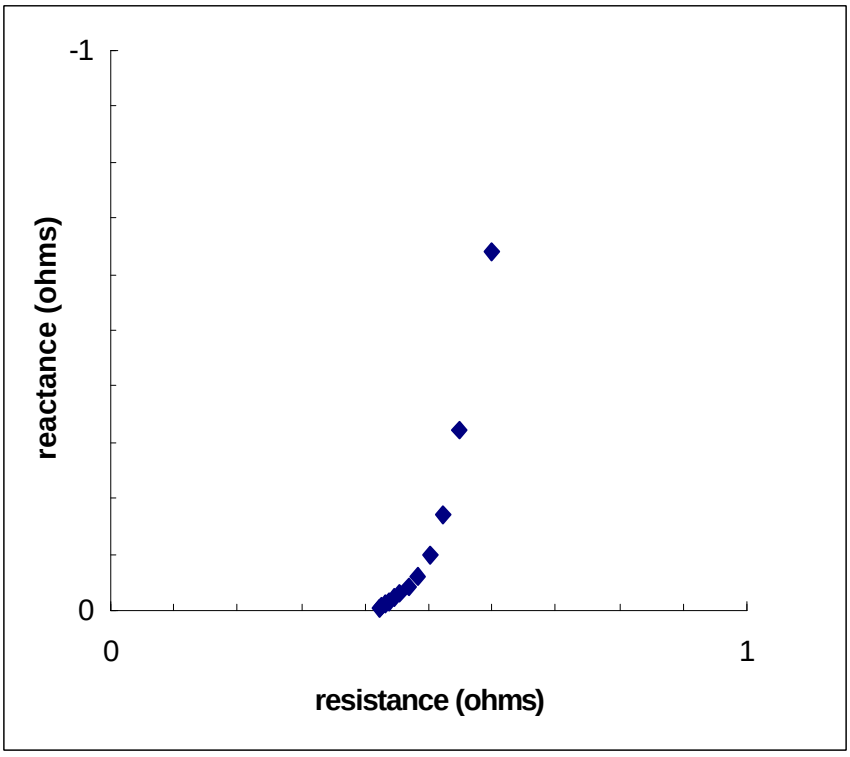

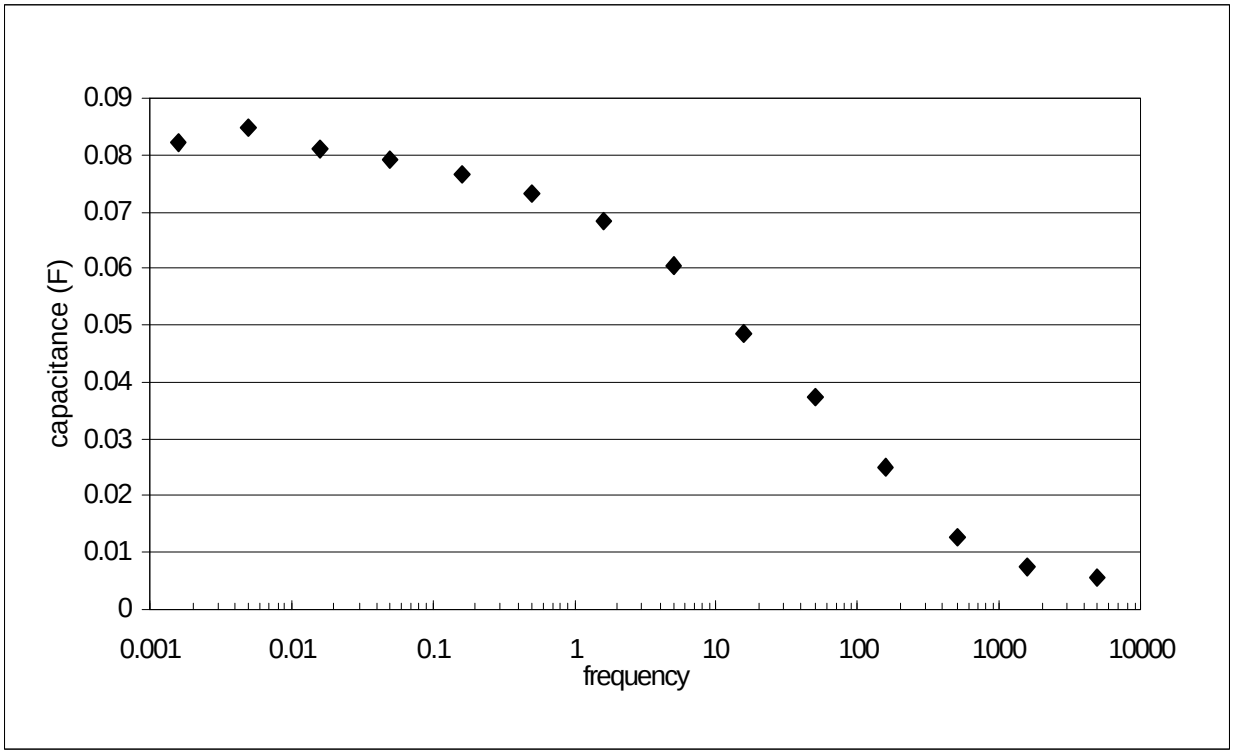

Figure 18. Capacitance vs. frequency for the shock-hardened tantalum hybrid capacitor. It is noteworthy that the "dc" capacitance is greater than twice the reported capacitance at 120 Hz.

Figure 19. Resistance vs. frequency for the shock-hardened tantalum hybrid capacitor.

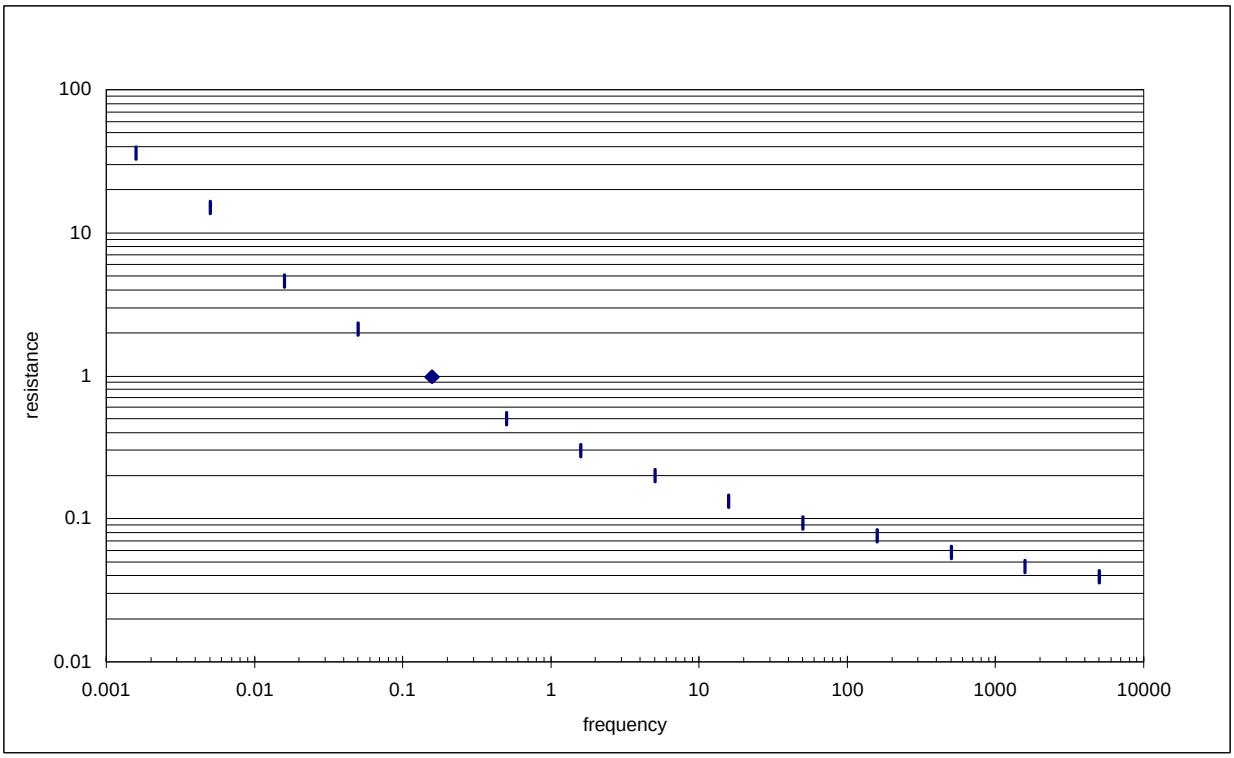

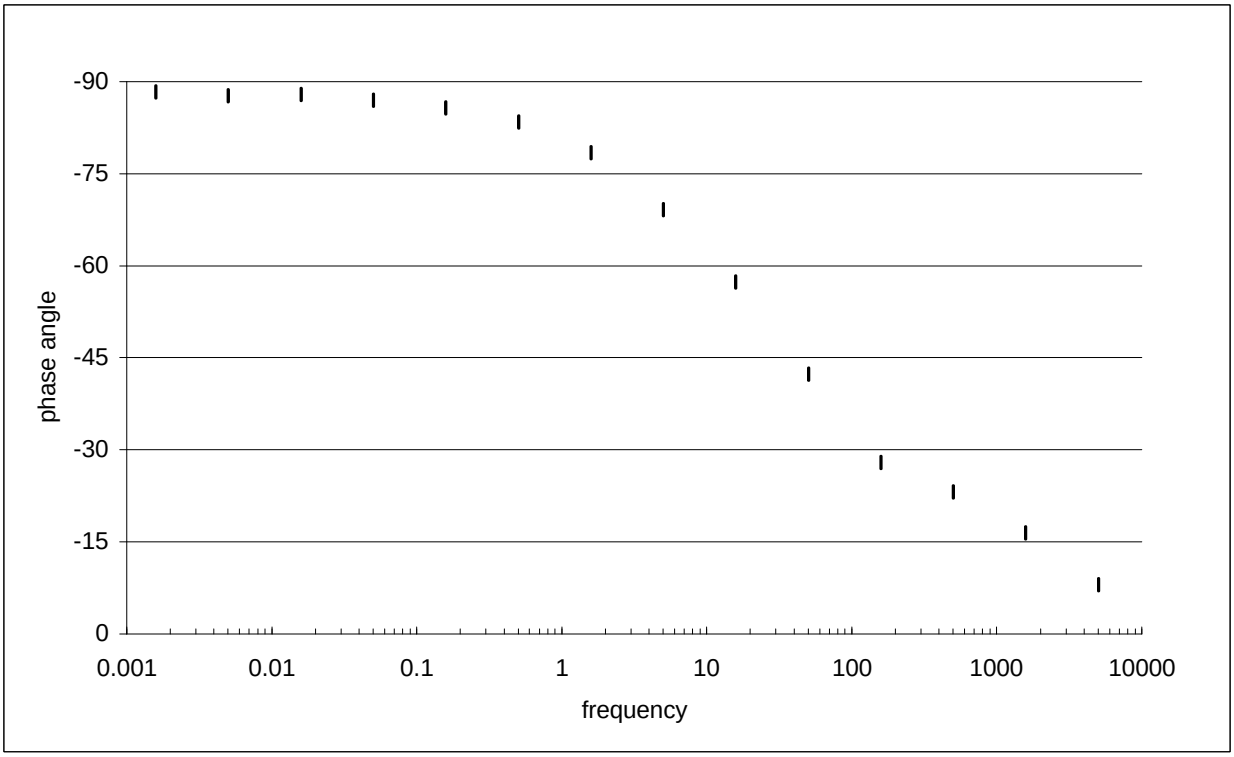

Figure 20. The above figure represents phase angle vs. frequency for the tantalum hybrid capacitor . The phase angle is between -85° and -90° from ~ 1 Hz down. This unit has a -45° phase angle at 65 Hz.

Figure 21. The figure to the right is a Nyquist plot of the impedance data. The plot intersects the x-axis at nearly 45°, indicative of the use of porous electrodes.

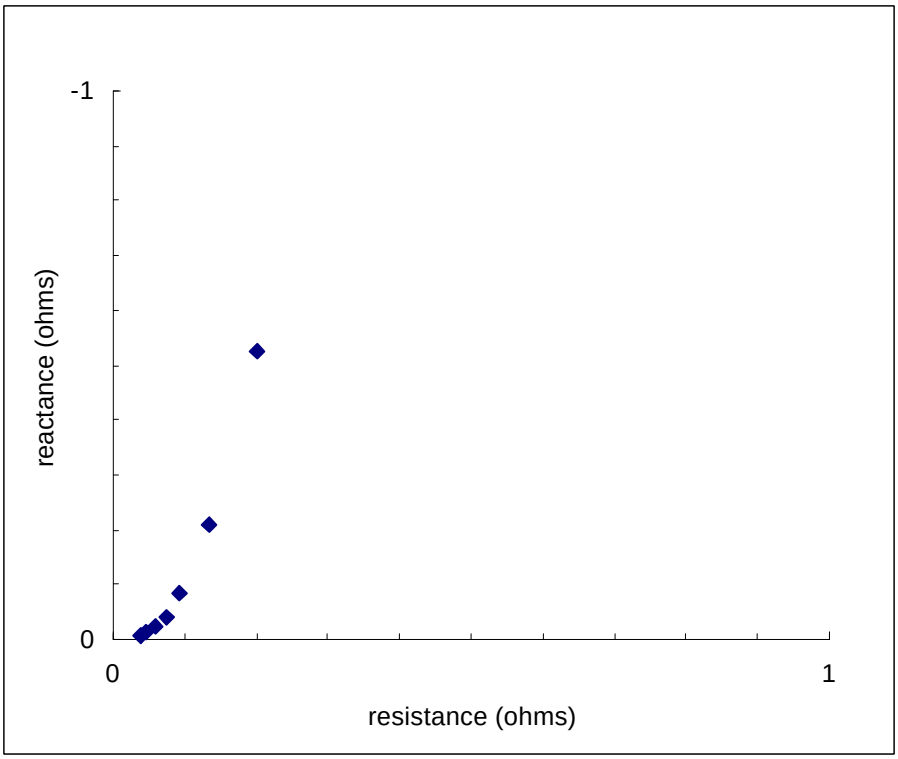

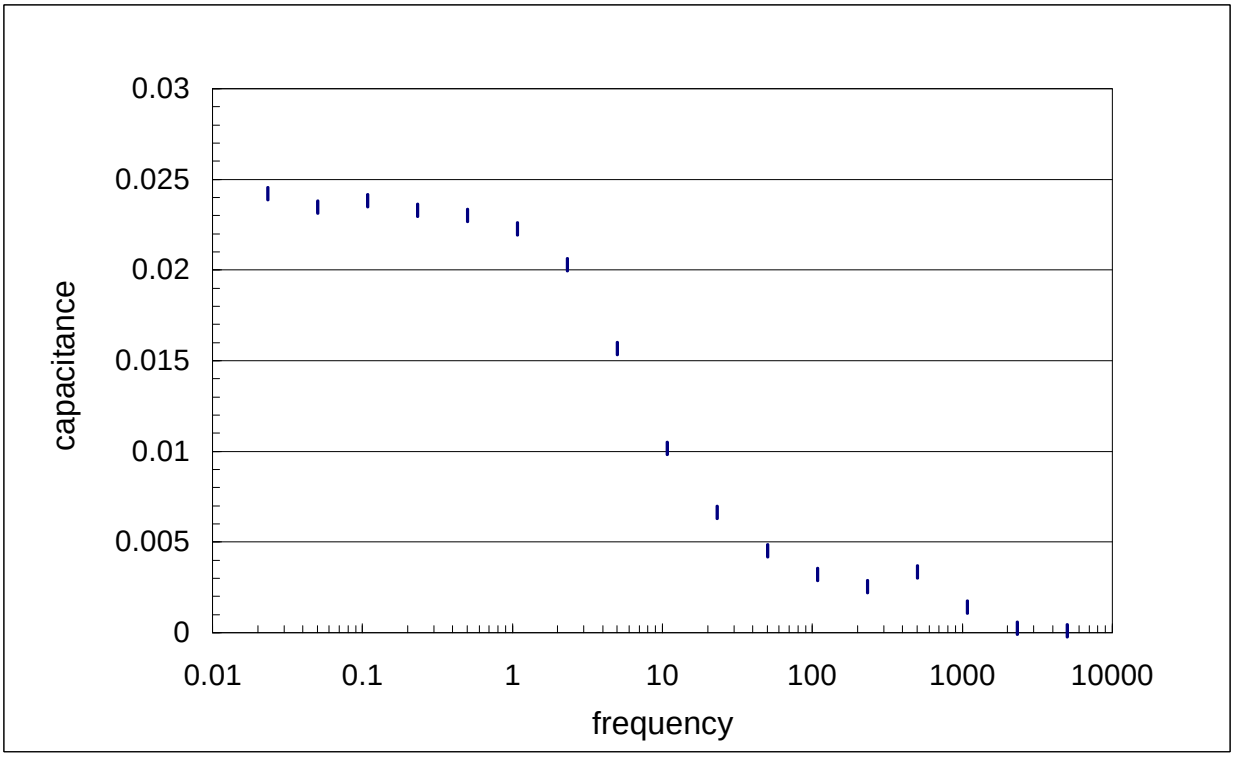

Figure 22 Capacitance vs. frequency for the aluminum hybrid capacitor. The high rate of change in capacitance with frequency has not been observed with tantalum capacitors.

Figure 23 Impedance vs. frequency for the aluminum hybrid capacitor. The data confirm a 0.995 ohm ESR measurement at 120 Hz.

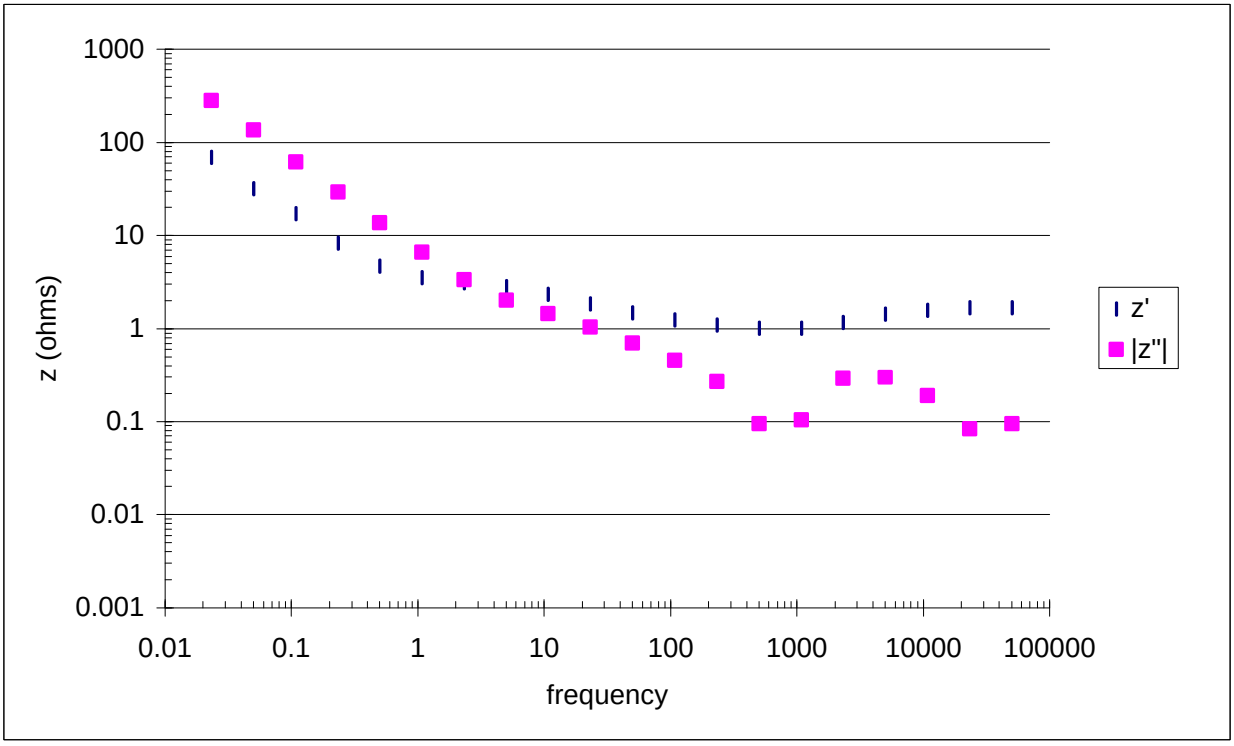

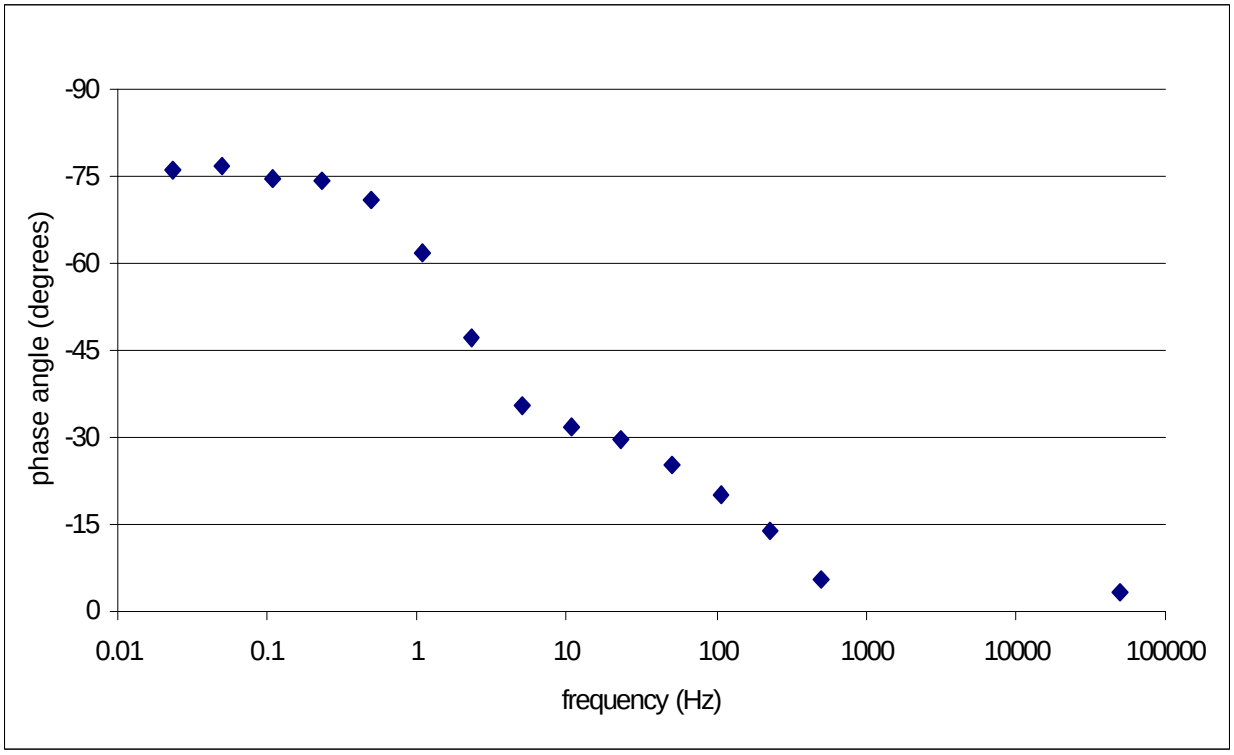

Figure 24. Phase angle vs. frequency for the aluminum hybrid capacitor. Behavior is influenced by the effects of high-resistance electrolyte.

Figure 25. Charge-discharge curve for the aluminum hybrid capacitor. The data correspond to a capacitance of 0.024 F. A constant current charge / load of 300 mA was applied. The voltage cycled between 3 - 28 volts. The period is 4.5 s.